Journal of Earthquake Engineering
Publication details, including instructions for authors and subscription information:
http://www.tandfonline.com/loi/ueqe20

Performance of degrading reinforced concrete frame systems under the Tohoku and Christchurch earthquake sequences

Adel E. Abdelnaby[a] & Amr S. Elnashai[b]

[a] Assistant Professor, Department of Civil Engineering, University of Memphis, 3815 Central Avenue Room 106C Engineering Science BLDG, TN, 38152, USA

[b] Nathan M. & Anne M. Newmark Endowed Chair, Department of Civil and Environmental Engineering, University of Illinois, 205 N Mathews Ave, Room 1114, Urbana, IL, 61801, USA

Accepted author version posted online: 22 May 2014.Published online: 22 May 2014.

To cite this article: Adel E. Abdelnaby & Amr S. Elnashai (2014): Performance of degrading reinforced concrete frame systems under the Tohoku and Christchurch earthquake sequences, Journal of Earthquake Engineering, DOI: 10.1080/13632469.2014.923796

To link to this article: http://dx.doi.org/10.1080/13632469.2014.923796

Performance of degrading reinforced concrete frame systems under the Tohoku and Christchurch earthquake sequences

Adel E. Abdelnaby[1)]

Amr S. Elnashai[2)]

1) *Assistant Professor, Department of Civil Engineering, University of Memphis, 3815 Central Avenue Room 106C Engineering Science BLDG, TN, 38152, USA, email: bdelnaby@memphis.edu, phone: 901 678-4633*

2) *Nathan M. & Anne M. Newmark Endowed Chair, Department of Civil and Environmental Engineering, University of Illinois, 205 N Mathews Ave, Room 1114, Urbana, IL, 61801, USA, email: aelnash@illinois.edu, phone: 217 265-5497*

The authors would like to acknowledge the financial and logistical contributions of the Mid-America Earthquake (MAE) Center, a National Science Foundation (NSF) Engineering Research Center funded under grant EEC-9701785.

Abstract

Field investigations after the recent Tohoku and Christchurch earthquakes reported failure of structural systems due to multiple earthquakes. In most failure cases the reported damage was mainly due to dramatic loss of stiffness and strength of structural elements as a result of material deterioration due to repeated earthquake loading. This study aims to investigate the degrading behavior of reinforced concrete frame systems subjected to Tohoku and Christchurch earthquake sequences. Numerical models of RC frames that incorporate damage features are established and inelastic response history analyses are conducted. The results presented in this study indicate that multiple earthquake effects are significant.

Keywords: Reinforced concrete, multiple earthquakes, damage accumulation, stiffness and strength degradation

1. Introduction

Problem statement

Reinforced concrete moment frames are used in many regions of high seismicity as earthquake force resisting systems. Frame structural components, such as beams, columns and beam-column joints are designed with adequate stiffness and strength to withstand the maximum seismic actions and deformations generated from imposed earthquake ground motions. However, during the recent Tohoku and Christchurch earthquakes, many reinforced concrete moment resisting frames experienced significant loss of stiffness and strength in their structural components, as a result of damage accumulation induced by repeated shaking. This was clearly observed for buildings that remained intact during the large mainshock (or earthquake of higher magnitude) and later collapsed in smaller aftershocks (or earthquakes of lower magnitudes). Since then, several studies investigating the degrading behavior of structures, including reinforced concrete moment resisting frame systems under multiple earthquakes, have been conducted.

Earthquake safety and resiliency of buildings have been extensively researched for structures subjected to one (most damaging) earthquake. Similarly, in design practice, buildings are designed to resist an earthquake of intensity level that corresponds to a code specific return period, assuming an initially undamaged building condition. This approach of design and assessment: (1) neglects the effects of accumulated damage resulted from previous small

earthquakes of shorter return periods than the design earthquake; and (2) does not consider the deterioration in stiffness and strength of structural components under multiple earthquakes or mainshock aftershocks sequences, especially in the case when structural retrofitting is not provided due to the short time frames between successive shaking (the case of Tohoku and Christchurch earthquakes).

Prior work aimed at investigating the response of structural systems subjected to multiple earthquakes has been conducted using simplified approaches due to the complexity of developing numerical models that accurately capture damage accumulation effects in terms of stiffness and strength degradation. Previous findings indicate that repeated shaking has a minimal effect on the response of structures in terms of peak displacements, maximum base shear and period elongation and hence it can be neglected for seismic evaluation of structures if the most damaging earthquake is to be considered. These findings contradict with the field investigations presented herein this paper after the March 11 Tohoku and Christchurch earthquakes.

Tohoku and Christchurch earthquakes

The Tohoku earthquake sequence, in Japan, generated more than 1,000 aftershocks of magnitudes 4+ (Figure 1). The most damaging aftershock (M_w 7.4) was reported on April 7, 2011. The epicenter of this aftershock was close to the Japanese shore; consequently it caused heavy damage and collapse of buildings in cities located near the shore, such as Sendai (Figure 2). It is worth noting that these buildings were slightly damaged after the mainshock on March 11.

The ongoing Christchurch earthquake sequence was initiated by the 7.0 magnitude Canterbury earthquake on September 4, 2010. Large magnitude earthquakes occurred later on (Figure 3), the most devastating earthquake nucleated underneath Christchurch on February 22, 2011. The latter earthquake caused more damage to structures and lifeline systems than the former although it was of a smaller magnitude.

Literature review

Previous research conducted on seismic performance of structures under repeated shaking has been conducted on Single Degree of Freedom (SDOF) and Multi Degree of Freedom (MDOF) systems. Due to their simplicity, SDOF systems incorporating inelastic hysteretic force-displacement relationships have been extensively used by many researchers such as Mahin (1980); Aschheim (1999); Amadio et al. (2003); and Hatzigeorgiou et al. (2009). MDOF systems such as moment resisting steel (Fragiacomo et al. 2003; Li et al. 2007; and Garcia et al. 2011) and concrete frames (Hatzigeorgiou et al. 2010) were also studied.

Effects of prior earthquake damage on the response of degrading SDOF systems were studied by Aschheim (1999). Takeda model (Takeda 1970) was used for the force-displacement hysteretic behavior (Figure 4). Prior damage was simulated by adjusting the initial stiffness as well as the current displacement ductility to reach a pre-specified level of prior ductility demand (PDD). The analytical results demonstrated that prior earthquake shaking has a very minor influence on peak displacement response. In addition, Aschheim indicated that the displacement response histories of damaged and undamaged systems, subjected to the same ground motions, match very well after the displacements reach their peak values. These findings were supported by the plot shown

in Figure 5 which represents the displacement response resulted from five SDOF systems of PDD values of 1, 2, 3, 4 and 8.

Hatzigeorgiou (2010) studied reinforced concrete frame systems using a bi-linear moment-rotation relationship at beam-column connections, beams and columns were assumed to behave elastically. Dynamic response history analyses were conducted on the frames and geometric nonlinearity were included. Hatzigeorgiou concluded that residual displacements play an important role on the stiffness degradation of the frames.

Due to the problem complexity of studying the multiple earthquake effects and capturing accurately the degrading behavior of structures, numerical models that have been used in literature were simplified as either system level (SDOF) or component level (MDOF with lumped plasticity at beam-column connections) based models. Modeling structures using idealized system and component level models leads to inaccurate assessment of their degrading response under repeated earthquakes; since many features are not precisely represented. The lacking features in the system level models include higher mode effects, localized failure behavior, and actions redistribution among structural components or assembly of components. While for component level models, the pre-specification of plastic hinge locations does not represent localized deformation in terms of plastic hinge length, yielding and buckling of steel, and crushing and cracking of concrete. In addition to using idealized models, prior research lacked proper selection criteria of earthquake ground motion sequences.

Objectives

The aim of this research is to clearly indicate that the response of degrading reinforced concrete frame systems is appreciably influenced by strong motion sequences in a manner that cannot be predicted from simple analysis, and is not reflected in current design provisions. To meet this objective, assessment of reinforced concrete frames is conducted by constructing numerical models that accurately capture the degrading behavior of reinforced concrete frame, and by using representative ground motion sequences.

To make a near-fully realistic assessment of the demands upon and performance of reinforced concrete structures subjected to repeated seismic loadings. A material level based model, as opposed to system and component based models, is established and used in conducting the assessment. The main challenge of establishing a degrading material level based model is that, in all existing analysis tools proper damage features of concrete and steel materials are not accounted for. This is due to the complexity of implementing these features in the material models since they (1) are computationally expensive; and (2) cause convergence problems when structures are subjected to complex dynamic loading. Furthermore, representative ground motions sequences are selected from the recent Tohoku and Christchurch earthquakes, and a comparison between the degrading and non-degrading models subjected to these ground motions is undertaken.

In addition to establishing a material level based model and selecting representative set of earthquake sequences, the scope of this study is extended to conducting a study on the response of reinforced concrete frame systems designed under different design criteria.

2. Model Development

Description and design of frames

The building under consideration is a 3-story, 2-bay (longitudinal) and 4-bay (transverse) reinforced concrete frame (Figure 6). This building is designed to support lateral loads using moment resisting reinforced concrete frame systems in both horizontal directions. The highlighted frame located on axis C is of interest in this study.

Three design concepts are introduced for the frame system, namely gravity, direct, and capacity design criteria. These design criteria are used to size the frame beams and columns and detail their adequate amount of steel reinforcement to resist imposed loads. Gravity load resisting frame is designed under the action of factored vertical dead and live loads only. Different loading configurations for live loads defined by the ASCE-07 code are used to maximize the design straining actions at critical sections. For the direct and capacity designed frames, seismic forces imposed on the systems are calculated based on ASCE-07 code, assuming the building is located in Aliso Vieji, California and it is on type B soil (S_{DS} = 0.989g and S_{D1} = 0.349g). The direct designed frame is designed with accordance to the requirements of ACI 21.1.2 and ACI21.2 for ordinary moment frames. A response modification factor (R) equals 3 is used. The capacity designed frame satisfies ACI 21.5 and ACI 21.6 for beams and columns, for special moment frames (R = 8). The equivalent static lateral load method is used to simplify the design procedure.

The beams and columns of the direct designed frame are dimensioned and reinforced to resist the locally evaluated actions (bending moment, shear and axial forces) with no due consideration to the action redistribution effects in the system as a whole. Therefore, the sections are solely designed to resist the imposed actions. The capacity designed frame deployed strong column weak beam method. In this method, the beams are considered the energy dissipative zones where flexural plastic hinges are favorably located at. Therefore, design straining actions of beams are evaluated from the applied actions. Design actions for columns are calculated based on the beam-column joints equilibrium taking into account all various sources of over-strength of beams sections. Detailing of longitudinal and transverse reinforcement is based on the ACI 2008 design code for reinforced concrete structures in high seismic regions. The design of frame sections and reinforcement detailing for the three frame systems are shown in Figure 7, Figure 8, and Figure 9, additional information can be found in Abdelnaby (2012).

Constitutive material models

Two modeling classes of the frame systems are presented. The first and second classes comprise the non-degrading and degrading frame systems, respectively. The non-degrading frame systems utilize commonly used material models in design and assessment of reinforced concrete frames, namely Mander model for concrete (Mander et al. 1988) and bilinear stress-strain relationship for steel.

For the degrading frame systems (class two), a plastic-damage model of concrete developed by Lee and Fenves (1998), and the modified Menegotto-Pinto steel model (Menegotto and Pinto 1973 & Gomes and Appleton 1996) are utilized. The models are implemented in the open source

Mid America Earthquake Center fiber-based finite element analysis software, Zeus-NL. The constitutive relationship of the concrete model is based on plasticity and continuum mechanics. The concept of fracture-energy-based multiple-hardening is used to represent tensile and compressive damage independently. A thermodynamically consistent scalar model is used to simulate the stiffness degradation and recovery. Stiffness recovery scheme is introduced to simulate crack opening and closure. In addition, the evolution of yield surface is controlled by the strength function of effective strength that accounts for strength deterioration due to existence of cracks parallel to the loading direction. Figure 10 shows the cyclic stress-strain relationship of concrete under tension and compression.

The modified Menegotto-Pinto steel model (shown in Figure 11) simulates the following characteristics: (1) elastic, yielding and hardening branches in the first excursion; (2) Baushinger effects which consists of (a) reduction of yield stress after a reverse which increases with enlargement of the plastic strain component of the last excursion; (b) decrease of the curvature in the transition zone between the elastic and the plastic branches; (3) isotropic strain which consists of an increase of the envelope curve, proportional to the plastic strain component of the last excursion; (4) fracture of reinforcing bars when the fracture strain is exceeded under any excursion; and finally (5) inelastic buckling of reinforcing bars after crushing of bar surrounding concrete. Figure 12 shows the cyclic stress-strain relationship of steel under tension and compression and highlights the main model features.

Fiber analysis

A detailed 2D fiber-based finite element model is established using 3D cubic elasto-plastic beam-column elements implemented in Zeus-NL software to model beams and columns. The software is capable of conducting static and dynamic analyses incorporating material and geometric non-linearity (employing the Eulerian formulation). A mesh of four elements is used for each beam/column member. To capture the high inelasticity induced near the beam-column joints accurately, smaller element sizes are used at the start and end points of each member. The length of elements is 0.15L, 0.35L, 0.35L, and 0.15L starting from the start to end points of the beam/column member respectively. The element sizes used in this study were determined based on a rigorous mesh sensitivity analysis of the frame subjected to constant gravity loads and monotonically increasing lateral loads. The mesh of the frame element is shown in Figure 13. This figure also describes the fiber analysis approach Zeus-NL utilizes.

The fiber-based finite element modeling, used in this study, is an efficient and accurate tool for simulating the response of a complete structural system under static and dynamic loading conditions. Members of the frame are modeled using elasto-plastic beam-column elements, with 200 monitoring points. These elements follow the Euler-Bernoulli formulation (Izzuddin and Elnashai 1993a, b). Each element has two nodes, for 2D analysis, each node considers 3 Degrees of Freedom (DOFs), two displacement components and one rotation. Evaluation of stiffness matrix of the element is performed at two Gaussian points located at a distance approximately 0.3l from the mid-point of the member. The section at each integration point is further divided into fibers that form the basis of distributed inelasticity models. Section stiffness is evaluated at

the Gaussian points based on the contribution of each fiber. Integration of the stiffness at the Gaussian points yields the tangent stiffness matrix for the element. The element stiffness matrices are assembled into the global stiffness matrix of the whole structure.

3. Ground Motion Sequences

Ground motion sequences from Tohoku and Christchurch earthquakes are used. Successive records at three stations from Japan and one station from New Zealand are collected and applied in series. Sequences ground accelerations from each station are subjected to the frame systems separately. A time buffer ranging from 10 to 20 seconds between repetitive earthquake records is enforced to ensure that the structure is brought to rest before it experiences the succeeding earthquake (Figure 14). Hence the structural behavior under succeeding earthquakes is not influenced by remaining dynamic movements occurring from preceding earthquakes.

Tohoku earthquake records

Tens of monitoring stations in japan experienced multiple earthquakes, each of which are of magnitude more than 5.5. Two stations are considered in this study, namely stations FKS013 and IWT007. The locations of these stations as well as the epicenter of the March 11 main shock and significant subsequent aftershocks are shown in Figure 15, additional information with regards to the stations can be found at http://www.k-net.bosai.go.jp/. Since thousands of records comprising the mainshock and aftershocks were monitored at each station, insignificant aftershock records of peak ground acceleration (PGA) less than 0.15g and spectral acceleration (at the natural

period of the structure) less than lowest spectral acceleration resulting from the earthquake ground motion sequence, are omitted to save analysis time.

Significant earthquakes measured at station FKS013 consisted of six records, which contain the main shock on March 11, 14:46 (record 1), and aftershocks on April 7, 23:32 (record 2), April 11, 17:26 (record 3), April 11, 17:58 (record 4), April 11, 20:42 (record 5), and April 12, 14:07 (record 6). The six records are plotted in series in Figure 16. Station IWT007: Similarly, acceleration time histories of significant records are selected and insignificant ones are omitted (Figure 16), therefore two records are only considered. The first record is the March 11 main shock and the second is the April 7 (M7.4) aftershock.

Ground motion characteristics of each individual record, measured at the two stations, are provided in terms of Peak Ground Acceleration (*PGA, g*), Peak Ground Velocity (*PGV, cm/sec*), Peak Ground Displacement (*PGD, cm*), maximum Velocity to maximum Acceleration ratio (*V/A, sec*), Arias Intensity (*AI*), Characteristic Intensity (I_c), Housner Intensity, Predominant period (T_p), and Mean Period (T_m), are shown in Table 1.

Christchurch earthquake records

Similar to the selection criteria of records followed in Tohoku earthquakes, significant records of high PGAs that correspond to large magnitude earthquakes in New Zeland are only considered. Subsequent earthquake records measured at station CBGS (Christchurch Botanic Gardens) are used, the records are obtained from (http://www.geonet.org.nz/resources/basic-data/strong-motion-data/). Table 2 shows the records date, time and magnitude. Nine significant earthquakes

of PGA>0.2g are monitored. The acceleration time history of the earthquake sequence is shown in Figure 17 along with the response spectra of each individual record. The records are defined by their local time of generation, see Table 2; for example the third record (on December 25, 2010) occurred at time 21:30:15 and its ID code is 213015 as shown in Figure 17. A summary of ground motion characteristics of individual records of Christchurch earthquake records measured at station CBGS is shown in Table 3.

4. Analysis Results

Eigen value analysis and fundamental periods

Eigen value analyses are conducted to investigate the modes of vibration and the fundamental periods of the three frame systems. Lumped masses were assigned at the nodes of beam elements. The masses are calculated based on 100% dead load and 25% live load. The first two natural periods of the structures are listed in Table 4. It is worth noting that the mode participation factor of first mode exceeded 90% for all three frames.

Pushover analysis

The pushover analysis is undertaken to shed light on design weaknesses of gravity and direct designed frames and to verify that the design concept of strong column weak beam approach is imposed on the capacity frame. Prior to starting the pushover analysis, the structure was subjected to constant gravity dead and live loads. After applying gravity loads, the frames were subjected to monotonically increasing lateral inverted triangle load pattern using force control up

to the peak point of the load-displacement curve. Post the peak point, response control loading phase is used to capture the softening (negative slope) behavior of the frames. This means that the software switches from force control to displacement control at the peak response. The response of the frame systems is monitored in terms of stiffness, strength and ductility of the three frame systems (Table 5). The capacity designed frame exhibited the highest global stiffness, strength and displacement ductility, the direct designed frame has the lowest ductility, and the gravity designed frame has the lowest stiffness and strength.

Location of plastic hinges and their formation pattern is provided in Figure 18. The gravity designed frame exhibited plastic hinges at columns only. Plastic hinges are initiated at the lower story of the direct designed frame resulting in an observed soft story behavior. While the capacity designed frame behaved as designed, plastic hinges are developed at beams first causing actions redistribution from beams to columns, leading to ductile failure behavior.

Comparison with non-degrading models predictions

The non-degrading and degrading gravity designed frame systems are subjected to the March 11 and April 7 Tohoku mainshock-aftershock sequence, measured at station IWT007. The response of both systems under the April 7 aftershock is monitored with (damaged systems) and without (undamaged systems) consideration of previous damage induced by the mainshock. For the damaged case, ground acceleration records of the mainshock and aftershock are applied to the systems in sequence, while for in the undamaged case, the aftershock acceleration records are only applied.

Top displacement response for the non-degrading and degrading gravity frame models are reported in Figure 19 and Figure 20 for the damaged and undamaged cases. A zoom in the response of the damaged and undamaged systems under the April 7 aftershock (from 315 to 330 seconds and plotted on top of each other) is provided to better compare the displacement amplitudes and periods for the damaged and undamaged systems.

The damaged response of the non-degrading frame under the April 7 aftershock matches very well with the undamaged frame response, post the peak displacement while the behavior prior to the peak displacement observes longer period and larger displacements. This is explained as follows: (1) the stiffness of the undamaged system at the peak displacement reaches its lowest value and stays constant throughout the whole earthquake sequence, since stiffness reduction in non-degrading models is influenced solely by the maximum displacement the system experiences; (2) P-Δ effects play a role on stiffness reduction and that explains the difference in the peak displacements.

For the degrading model, the displacements under the April 7 aftershock for the damaged and undamaged cases are discrepant (Figure 20). Longer periods and larger displacement amplitudes are revealed for the damaged system; in addition higher residual displacements are monitored for the damaged case. In summary, a totally different response is predicted for the gravity designed frame under the April 7 aftershock if the damage effects of the main shock are considered in the analysis when the degrading models are used. This highlights the importance of including damage dependent models in studying the effects of multiple earthquakes shaking on the response of structures. The results described confirm that non-degrading models cannot

accurately predict the response of structures under more than one earthquake. Hence further analyses in this study are conducted using the degrading models only.

Response of degrading frame systems

The gravity frame is subjected to the Christchurch earthquake sequence using records measured at station CBGS. Two cases are considered in the analysis. The first case (case 1) considers all nine records measured at the station while the second case (case 2) excludes prior shaking of the first three records and considers only the last six records. The inter-story drifts are plotted in Figure 21. In case 1, the analysis was not completed due to convergence problems that occurred during the fourth record. This convergence was caused due to excessive drifts, which exceeded 10%, at the first story. In case 2, the analysis under the fourth to ninth records series converged and a maximum drift of 3.04% is reported at the first story. These results ensure that the effects of prior shaking of the first, second and third records caused the complete collapse of the first story of the gravity frame system during the application of the forth record. However, when prior shaking effects are not considered, the frame withstood the forth earthquake as well as all the subsequent earthquakes in the sequence.

The response of the direct designed frame under the Tohoku earthquake sequence is also presented. Significant records measured at station FKS013 are used. The sequence consists of six records, 1 to 6, of PGAs of 0.36g, 0.37g, 0.15g, 0.19g, 0.11g, and 0.31g. The first, second and sixth earthquakes are the most devastating ones within the sequence since they have the highest PGAs and correspond to earthquakes of high magnitudes (Figure 16). Figure 22 shows the inter-story drifts of the direct frame, the maximum first story drifts reported for records 1, 2, and 6 are

0.89%, 1.48%, and 1.15%. It is worth noting that the maximum first-story drift reported during record 6 is higher than the drift reported during record 1; however record 1 has a higher PGA almost 1.2 times the PGA of record 6.

The top displacements of the direct designed frame are compared for the undamaged and damaged cases under record 2. For the damaged case, effects of prior shaking due to record 1 is considered, while for the undamaged case, record 2 is applied to the frame in its initial state. The top displacements for the damaged and undamaged frames are plotted on top of each other as shown in Figure 23. The plot shows a similar response of both cases within time frames of 290-295 and 304-308 seconds, however discrepancies are revealed between the 295 and 304 seconds as well as 308 and 320 seconds.

The capacity frame is subjected to Tohoku earthquake sequence measured at station IWT007. Two significant records are used in the analysis; the first comprises the March 11 main shock and second comprises the April 7 aftershock. Inter-story drifts of the first, second and third floors are plotted in Figure 24. Higher drifts are observed during the April 7 aftershock due damage induced by the main shock.

A comparison between the initially damaged and undamaged frames is conducted. Figure 25 shows the top displacements of both frames. Fewer discrepancies are observed for the capacity frame response in the damaged and undamaged state in terms of overall frame displacement response (compared to the response of the gravity and direct designed frames). However, the maximum top displacement reported for the damaged frame under the April 7 aftershock is 37.63 mm at time 18.00 seconds measured from the beginning time of the aftershock record. For the

undamaged frame, the maximum top displacement occurred at time 18.23 seconds and its value is 30.36 mm. Large residual displacements are observed for the damaged case, due to the mainshock.

5. Analytical Investigation

A comparison between the results of the gravity, direct and capacity designed frames is undertaken. Christchurch records are subjected to the three frame systems. The results are provided in terms of maximum top displacements and number of plastic hinges experienced during each individual record.

Top displacements

In order to compare the damaged and undamaged systems response, nine sequences are considered in the analysis. The first sequence (denoted by sequence 1 at legend of Figure 26) comprise record number 9 only (in this case prior damage due to records 1 to 8 is not considered), the third sequence (3) consists of records 7, 8 and 9 in series, while the ninth sequence (9) considers the whole sequence starting with records 1 and ending with 9, and so on and so forth. The top displacements of the frame systems under the nine earthquake sequences are shown in Figure 26.

The results show that highest displacements are reported at the gravity frame and lowest by the capacity frame. The gravity frame under sequence 1 showed similar maximum displacements during record 9, when prior shaking effects due to records 5, 6, 7 and 8 are considered

(earthquake sequences 1, 2, 3, 4, and 5). However, earthquake sequences 6, 7, 8 and 9 showed higher maximum displacements at record 9. It is worth noting that the maximum displacement at record 9 due to sequence 5 is equal to 70.83 mm while it is equal to 201.29 for sequence 9. Similar observations are revealed for the direct frame.

Unlike the gravity and direct frames, the capacity designed frame maximum top displacements at record 9 due to sequences 1 and 9 are equal to 12.53 mm and 17.00 mm respectively. The maximum displacement for the damaged case is almost 1.36 times their damaged counterparts, while for the gravity frame damaged displacement is 3.40 the undamaged one.

Plastic hinges

Similarly, plastic hinge formation at the ends of beam and column elements is also monitored for individual records of Christchurch earthquake sequence, measured at station CBGS. A plastic hinge is formed when the strains of the reinforcing bars at the sections located at a distance d/2 from the perpendicular element centerline exceed the yield strain of steel; where d is the depth of the perpendicular element as shown in Figure 27.

The number of plastic hinges is reported in Figure 28 for the gravity, direct and capacity frames. The maximum numbers of plastic hinges developed in three frame systems are, 24, 26, and 21 for gravity, direct and capacity frames. For the capacity designed frame, the number of plastic hinges keeps on developing by increasing the number of applied ground motions. This means that the capacity designed frame was able to absorb and dissipate more energy under earthquake

sequences, unlike gravity and direct designed frames where localized failure prevented force distribution among frame components.

6. Conclusions

The seismic performance of reinforced concrete frame systems, of different design approaches, subject to repeated strong motions is assessed. The response of damaged and undamaged systems is compared using commonly used material models as well as steel and concrete models of degrading features. Based on the analysis results it is shown that multiple earthquake effects have significant impact on the behavior of reinforced concrete structures in a manner that cannot be predicted from simple analysis (conducted using commonly used models for design and assessment of reinforced concrete structures). Moreover, this research confirms that the degrading response is not accurately captured based on simplified system level or component level models, that include damage features, presented in previous studies, this lead to reversing previous work recommendation. While three frame systems and four sequences of ground motions are considered in this study, future research should focus on providing detailed guidelines for design of structures located in regions prone to multiple earthquakes.

Based on analytical investigation, the capacity designed frame proved to perform better than gravity and direct designed frames, when subjected to earthquake sequences. Capacity designed frame response revealed formation of larger number of plastic hinges (most of the hinges are developed at beam ends), compared to gravity and direct frames. This allows the capacity designed frame to redistribute seismic forced among the frame components and behave in a

ductile manner throughout the while earthquake sequence; in addition it limits the inter-story drifts and displacements. On the other hand, soft-story behavior, and high residual displacements after individual earthquakes were observed for the gravity and direct designed frames, due to that localized degradation of columns stiffness and strength.

The results in this study and the conclusions drawn from them point towards the necessity of conducting detailed and comprehensive analyses of different structural systems using robust models to parametrically quantify the effect of multiple earthquakes on seismic response metric. The outcome from such parameterization could then be used to formulate design procedures that result in levels of structural safety for systems subjected to more than one earthquake that are consistent with current levels of safety in earthquake engineering design codes. In general, the analytical evidence presented in this paper highlight the potential of damage accumulation effects of structures in regions prone to multiple earthquake hazards.

References

Abdelnaby, A. E. (2012). “Multiple earthquake effects on degrading reinforced concrete structures.” *Ph.D. Dissertation, University of Illinois at Urbana-Champaign, IL, USA*.

ACI 318, *Building Code Requirements for Structural Concrete*, ACI 318-11, American Concrete Institute, Detriot (2011).

Amadio, C., Fragiacomo, M., and Rajgelj, S. (2003). "The effects of repeated earthquake ground motions on the non-linear response of SDOF systems." *J. Earthquake Engineering and Structural Dynamics*, 32, 291-308.

American Society of Civil Engineers (ASCE 7-05) and Structural Engineering Institute (SEI) (2005). *Minimum design loads for buildings and other structures*. Reston, VA, American Society of Civil Engineers/Structural Engineering Institute.

Aschheim, M., and Black, E. (1999). "Effects of prior earthquake damage on response of simple stiffness-degrading structures." *J. Engineering Spectra*, 15(1), 1-24.

Fragiacomo, M., Amadio, C., and Macorini, L. (2004). "Seismic response of steel frames under repeated earthquake ground motions." *J. Engineering Structures*, 26, 2021-2035.

Garcia, J., and Manriquez, J. (2011). "Evaluation of drift demands in existing steel frames as-recorded far-field and near-filed main shock-aftershock seismic sequences." *J. Engineering Structures*, 33, 621-634.

Gomes, A., and Appleton J. (1996). "Nonlinear cyclic stress-strain relationship of reinforcing bars including buckling." *J. Engineering Structures*, 19(10), 822-826.

Hancock J, Bommer JJ., (2006). "A state-of-knowledge review of the influence of strong-motion duration on structural damage." *Earthquake Spectra*, 22, 827-845.

Hatzigeorgious, G. (2010). "Behavior factors for nonlinear structures subjected to mutiple earthquakes." *Computer and Structures,* 88, 309-321.

Hatzigeorgious, G., and Beskos, D. (2009). "Inelastic displacement ratios for SDOF structures subjected to repeated earthquakes." *J. Engineering Structures*, 31, 2744-2755.

Hatzigeorgious, G., and Liolios, A. (2010). "Nonlinear behavior of RC frames under repeated strong motions." *Soil Dynamics and Earthquake Engineering*, 30, 1010-1025.

Ibarra LF, Medina RA, Krawinkler H., (2005). “Hysteretic models that incorporate strength and stiffness deterioration.” *J. Earthquake Engineering & Structural Dynamics*, 34, 1489–1511.

Iervolino I, Manfredi G, Cosenza E., (2006). “Ground motion duration effects on nonlinear seismic response.” *J. Earthquake Engineering & Structural Dynamics*, 35, 21–38.

Izzuddin, B. A., and Elnshai, A. S. (1993a). “Adaptive space frame analysis, part ii: a distributed plasticity approach.” *Proceedings of the Institution of Civil Engineers, Structures and Buildings,* 99, 317-326.

Izzuddin, B. A., and Elnshai, A. S. (1993b). “Eulerian formulation for large-displacement analysis of space frames.” *Journal of Engineering Mechanics,* 119(3), 549-569.

Lee, J., and Fenves, G. (1998). "Plastic damage model for cyclic loading of concrete structures." *J. Engineering Mechanics*, 124(8), 892-900.

Li, Q., and Ellingwood, B. (2007). "Performance evaluation and damage assessment of steel frame buildings under main shock-aftershock earthquake sequences." *J. Earthquake Engineering and Structural Dynamics*, 36, 405-427.

Mahin, S., (1980). “Effects of duration and aftershocks on inelastic design earthquakes.” P*roceedings of the Seventh World Conference on Earthquake Engineering, Istanbul,* vol. 5, 1980, pp. 677–80.

Mander, J. B., Priestley, M. J. N., and Park, R., (1988). “Theoretical stress-strain model for confined concrete.” *Journal of Structural Division, American Society of Civil Engineering,* 114, 1804-1826.

ACCEPTED MANUSCRIPT

Menegotto, M., and Pinto, P. E. Method of Analysis for Cyclically Loaded Reinforced Concrete Plane Frames Including Changes in Geometry and Nonelastic Behavior of Elements under Combined Normal Force and bending. In Proc. IABSE Symposium on Resistance and ultimate Deformability of Structures Acted on by Well-Defined Repeated Loads (Lisbon, 1973).

Ruiz-Garcia J., (2010). "On the influence of strong-ground motion duration on residual displacement demands." *Earthquake and Structures*, 1, 327–344.

Takeda, T. M., Sozen, M. A., and Nielson, N. N., (1970). "Reinforced concrete response to simulated earthquakes." *Journal of Structural Division, American Society of Civil Engineering,* 96, no. ST12, December.

Figure 1: Epicenter locations of mainshock (*yellow*) and aftershocks (*red*) in Tohoku earthquake, Japan (USGS); i.e. circle size denotes the magnitude of earthquake.

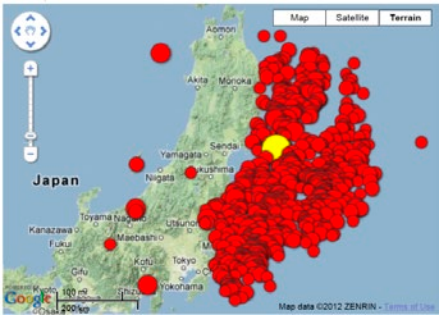

Figure 2: House collapsed in Sendai after the April 11 aftershock (Asahi-Shimbun, Japan; URL: http://www.asahi.com/special/gallery_e/view_photo_feat.html?jisin-pg/TKY201104120069.jpg).

Figure 3: The Christchurch earthquake sequence and magnitude.

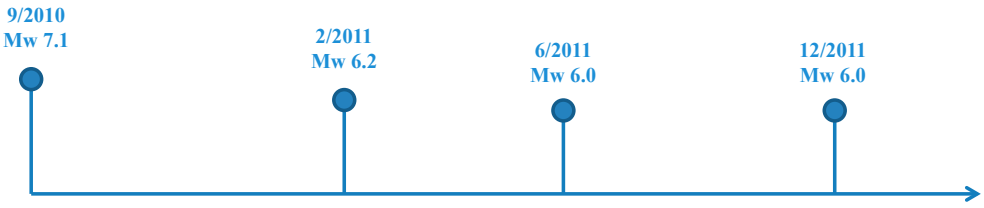

Figure 4: Modified Takeda model for SDOF systems incorporating pinching and strength degradation (used in Aschheim 1999).

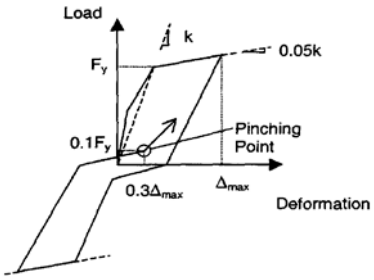

Figure 5: Displacement histories, for the first 40 (*up*) and 10 seconds (*down*) of the record, of oscillators having prior damage given by PDD = 0, 1, 4, and 8 (Aschheim 1999).

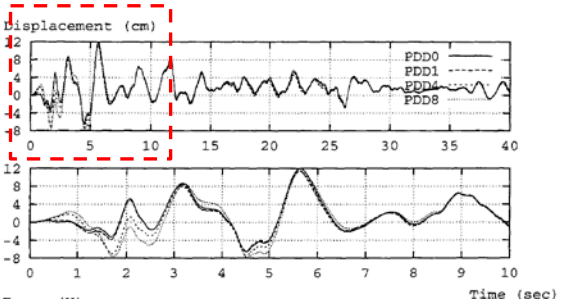

Figure 6: Plan and elevation of the studied building.

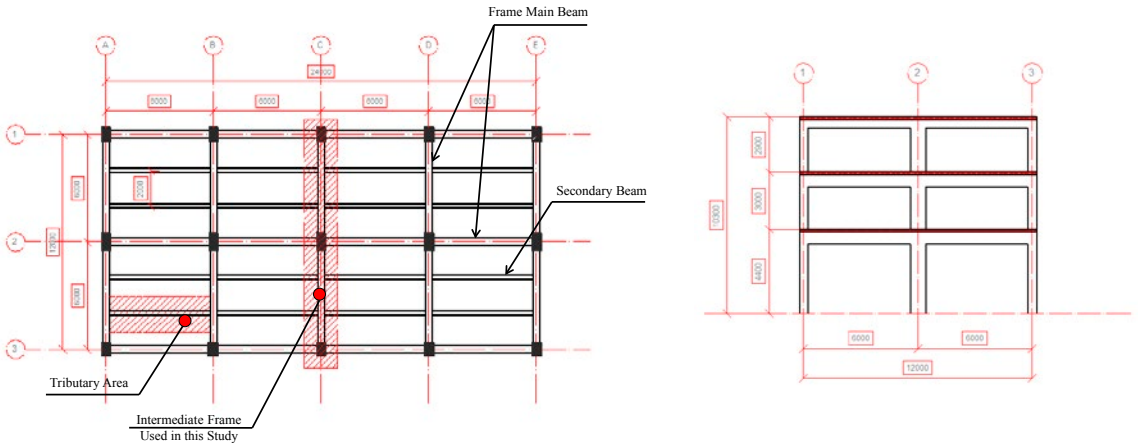

Figure 7: Gravity frame flexure and shear reinforcement (all longitudinal bars are # 7 and all stirrups are # 3 bars).

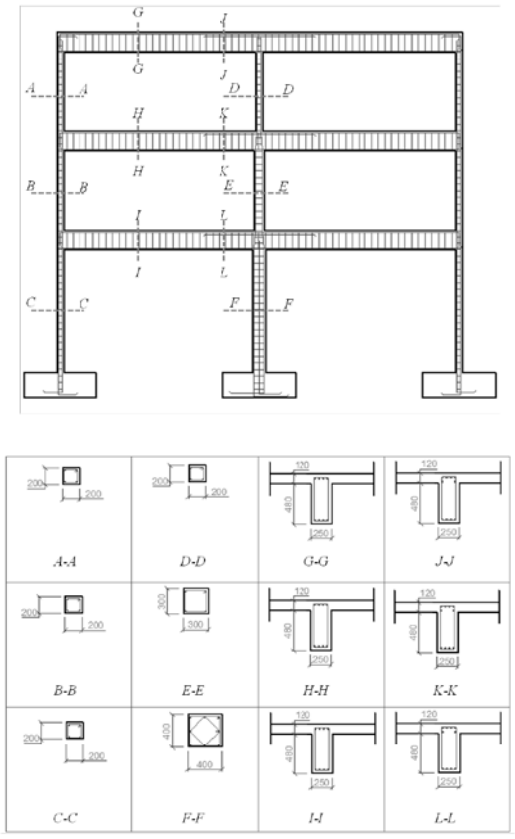

Figure 8: Direct frame flexure and shear reinforcement (all longitudinal bars are # 7 and all stirrups are # 3 bars).

\

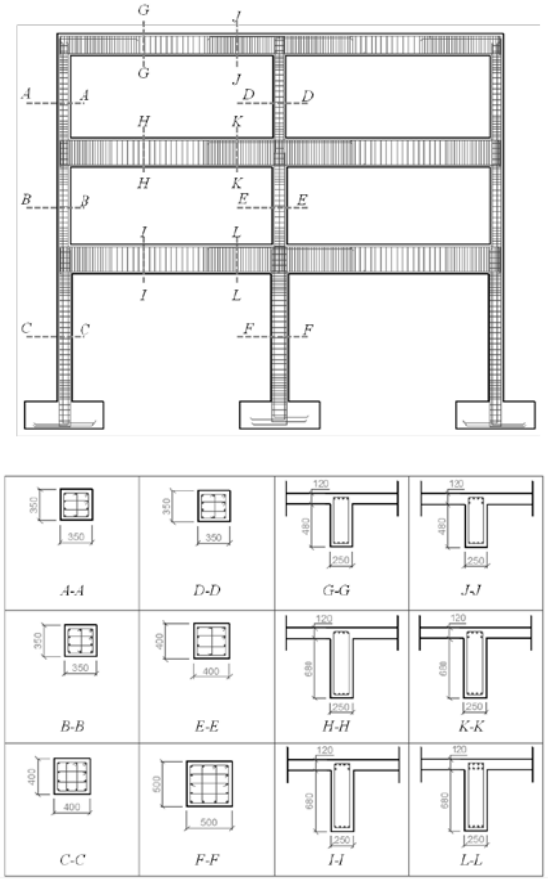

Figure 9: Capacity frame flexure and shear reinforcement (all longitudinal bars are # 7 and all stirrups are # 3 bars).

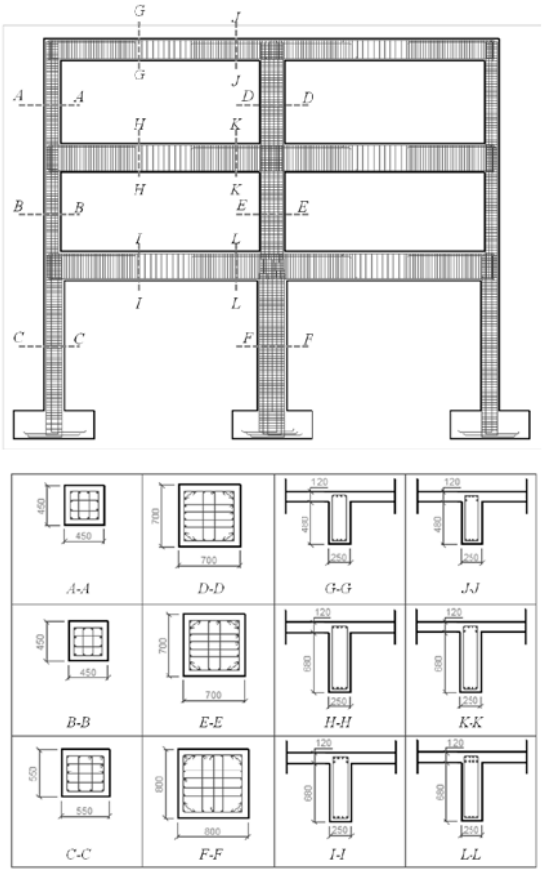

Figure 10: Uniaxial cyclic behavior of implemented degrading concrete model.

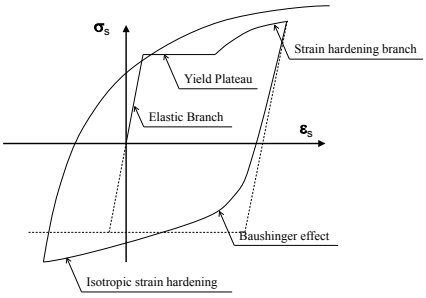

Figure 11: Main characteristics of steel stress-strain relationship (Gomes, 1997).

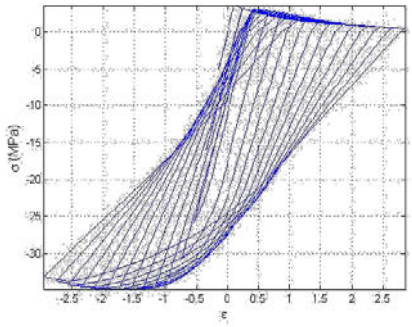

Figure 12: Buckling and fracture of implemented steel model in Zeus-NL (Abdelnaby 2012).

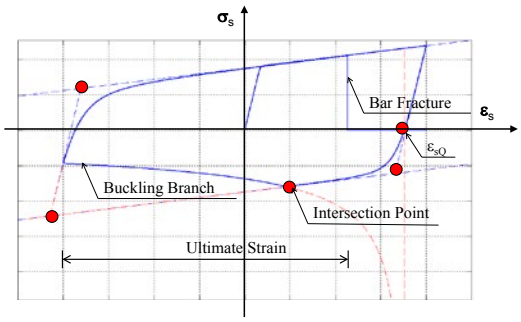

Figure 13: Fiber-based finite element model.

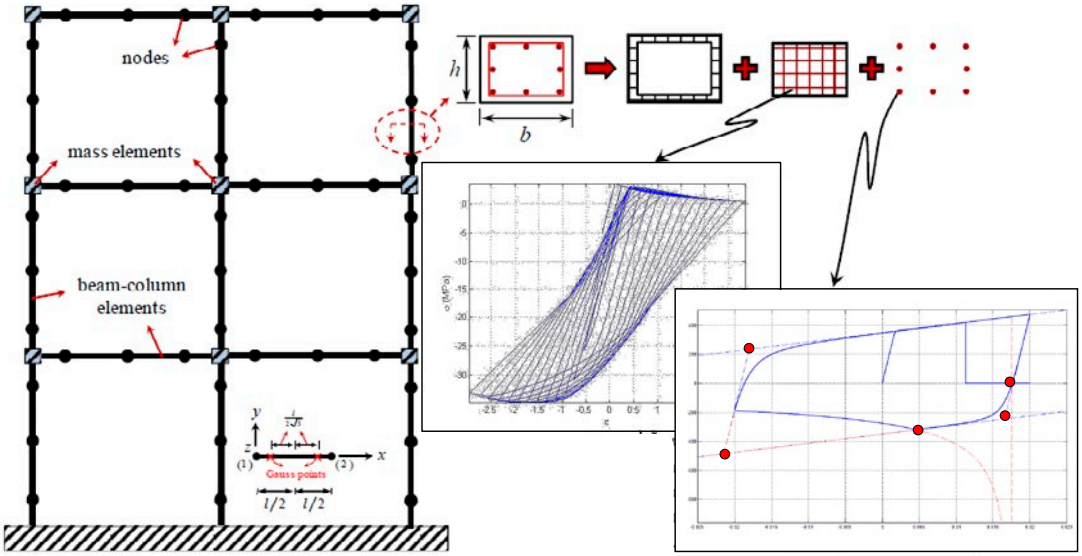

Figure 14: Time buffer between successive earthquakes to ensure that the structure is brought to rest.

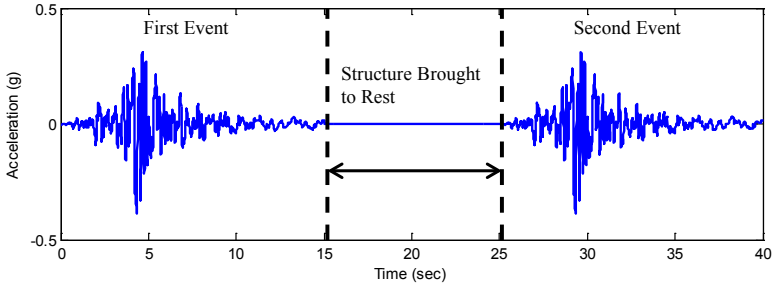

Figure 15: Epicenter location of significant earthquake measured at stations (a) FKS013, and (b) IWT007; square size denotes the magnitude.

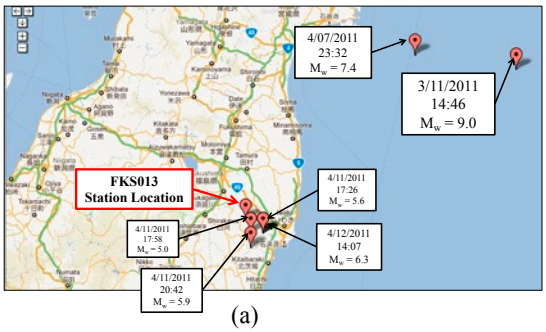

(a)

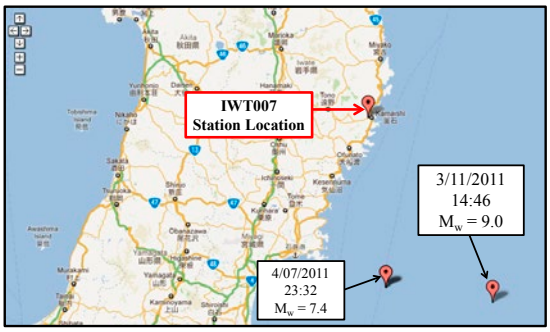

(b)

Figure 16: Acceleration time histories at stations (a) FKS013; and (b) IWT07.

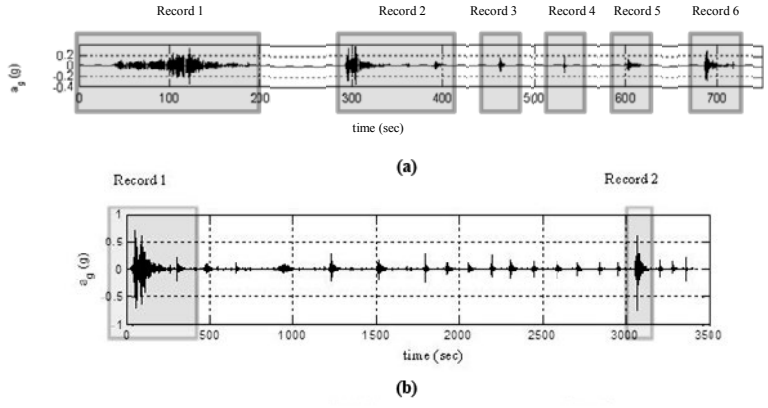

Figure 17: Earthquake sequence at station CBGS in New Zealand, and the response spectrum of each individual record.

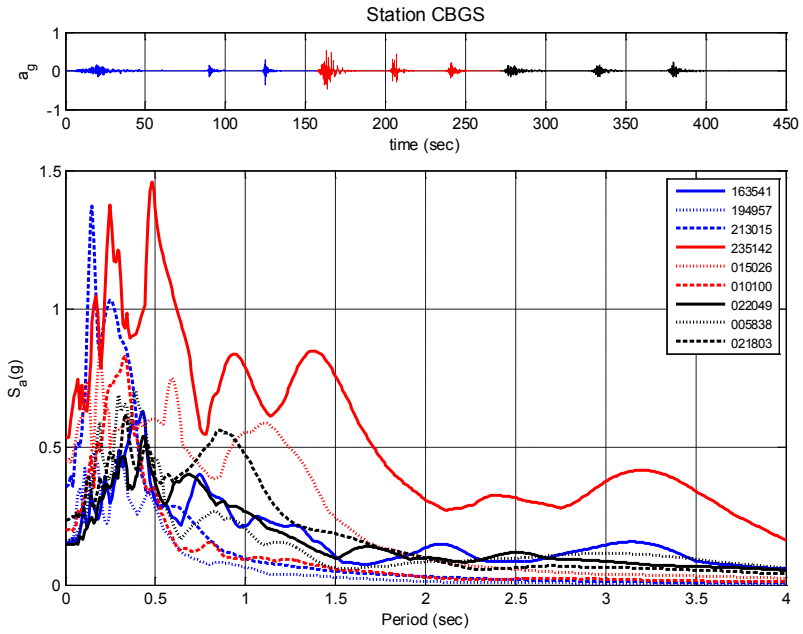

Figure 18: Plastic hinges in frame systems, i.e. the numbers indicate the sequence of plastic hinges formation with respect to load steps; (*a*) gravity, (*b*) direct, and (*c*) capacity designed frames.

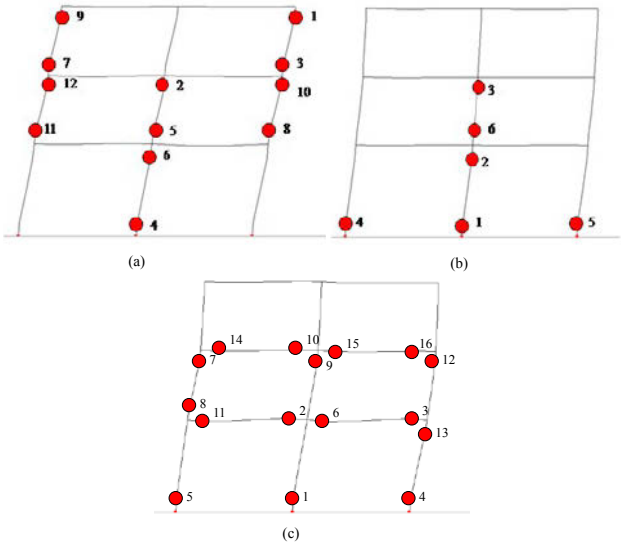

Figure 19: Top displacements monitored for the non-degrading gravity frame model under (a) two and (b) one earthquakes; and (c) a comparison of damaged and undamaged response.

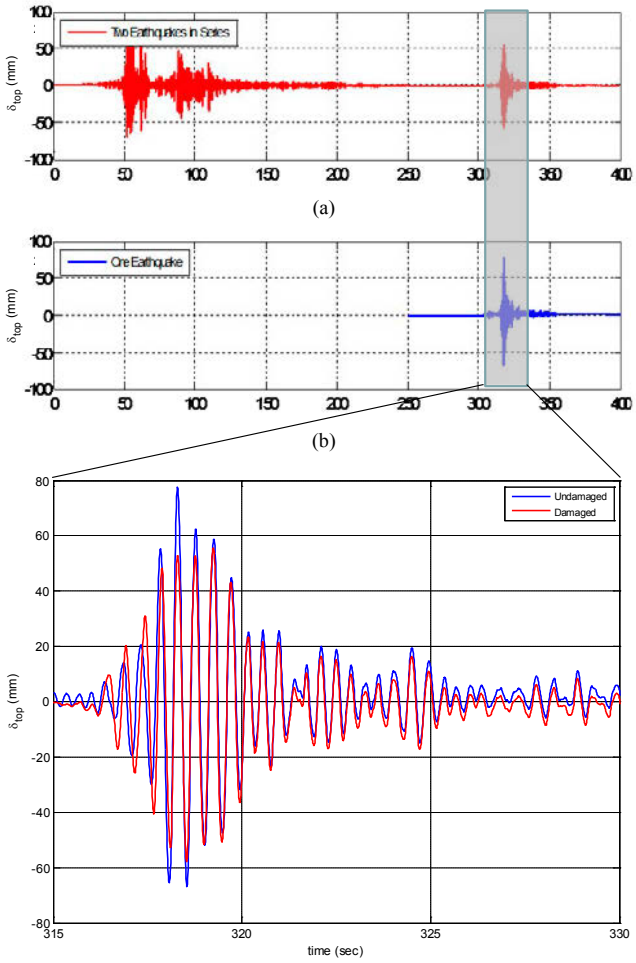

(a)

(b)

(c)

Figure 20: Top displacements monitored for the degrading gravity frame model under (a) two and (b) one earthquakes; and (c) a comparison of damaged and undamaged response.

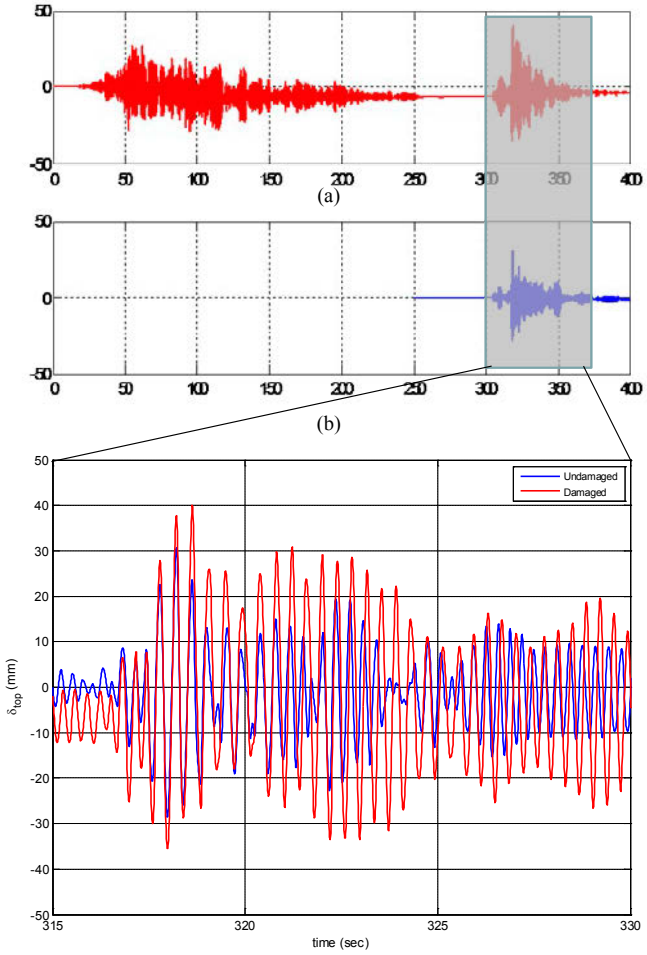

(c)

Figure 21: Inter-story drift of the gravity frame under earthquake sequence measured at station CBGS in the Christchurch earthquake; response of the frame under the whole earthquake sequence (*up*); response of the frame under the last six records only (*down*).

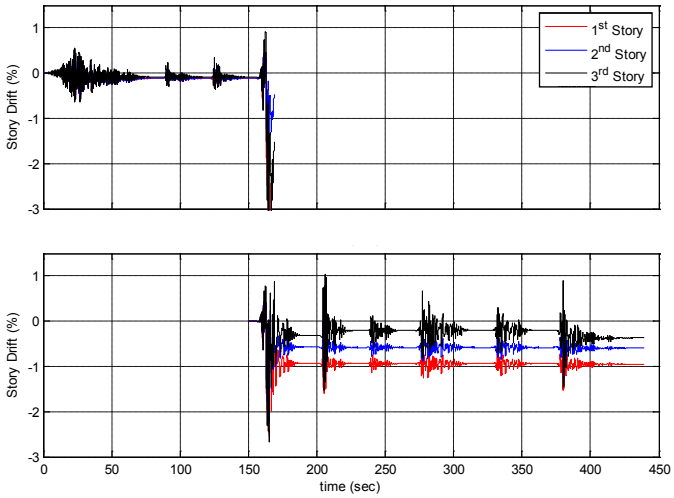

Figure 22: Inter-story drifts of direct frame under Tohoku earthquake sequence measured at station FKS013.

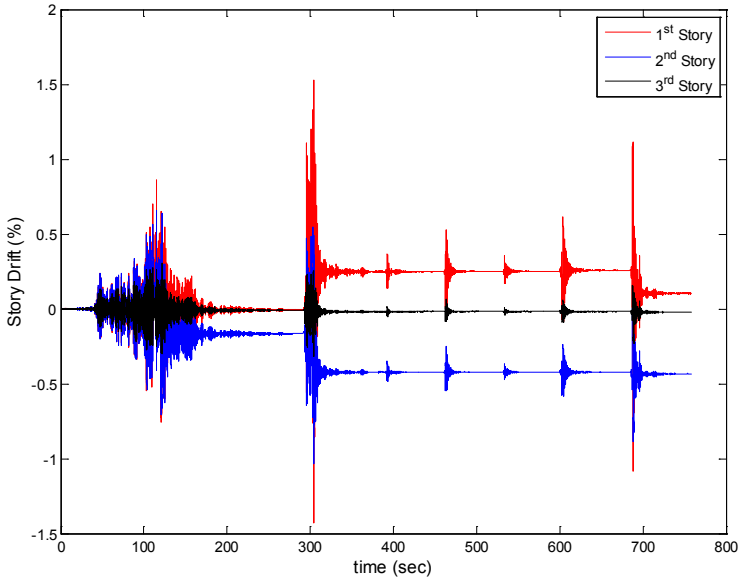

Figure 23: Top displacements monitored for the damaged and undamaged direct frames under record 2 of FKS station, Tohoku earthquake sequence.

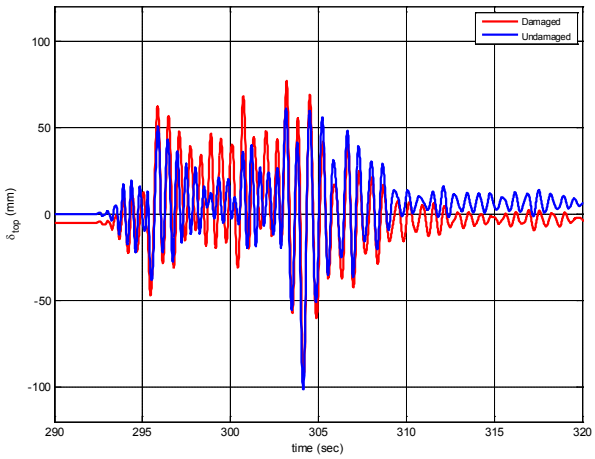

Figure 24: Inter-story drifts of the capacity frame under Tohoku earthquake sequence, station IWT007.

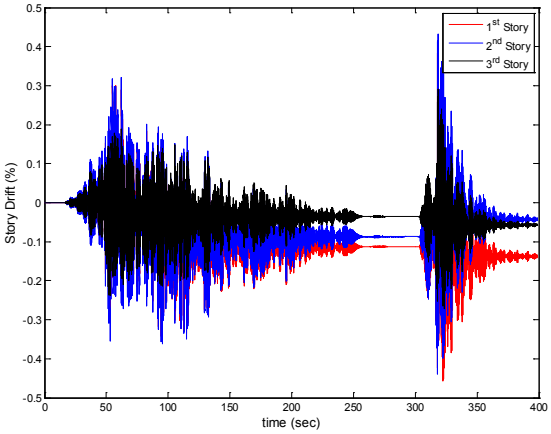

Figure 25: Top displacements of the damaged and undamaged frames under the April 7 aftershock, station IWT007.

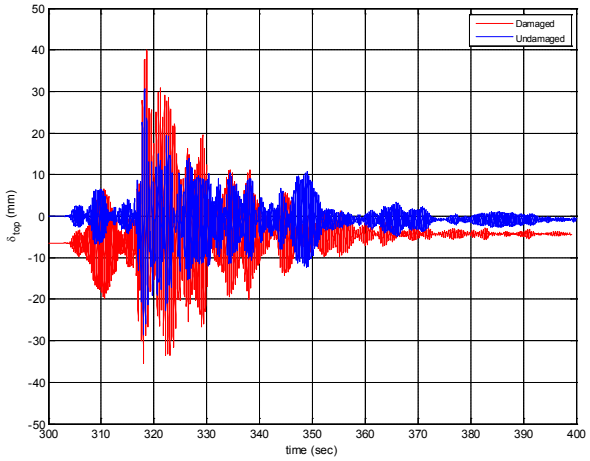

Figure 26: Maximum top displacements of (a) gravity, (b) direct, and (c) capacity designed frames under selected sequences of CBGS records.

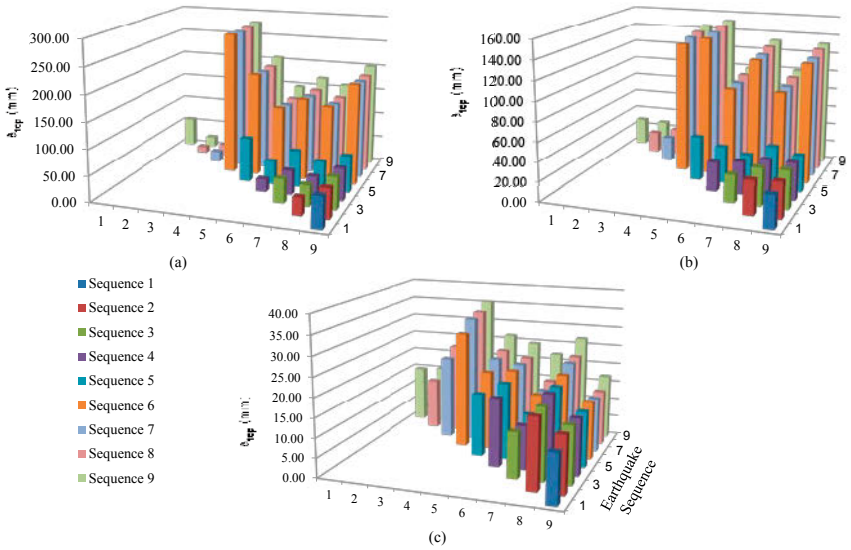

Figure 27: Beam-column joint, figure shows reinforcing bars where strains are monitored at (marked in red).

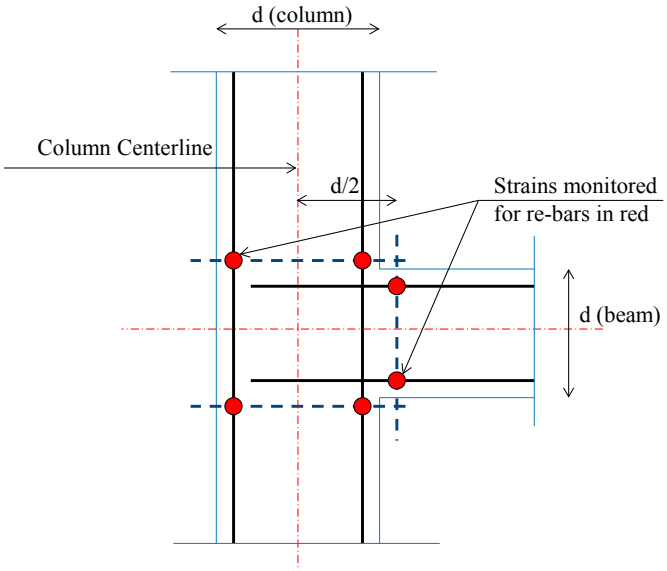

Figure 28: Plastic hinges formation for (a) gravity, (b) direct, and (c) capacity designed frames, under the Christchurch earthquake sequence (station CBGS).

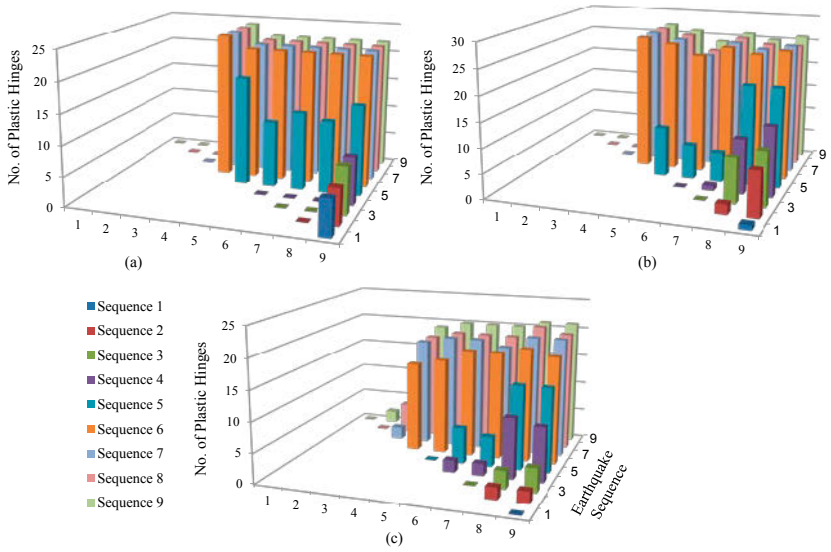

Table 1: Ground motion characteristics of individual records at stations FKS013, and IWT007.

	FKS013							IWT007	
Parameter	**1**	**2**	**3**	**4**	**5**	**6**	**Parameter**	**1**	**2**
PGA	0.36	0.37	0.15	0.19	0.11	0.31	**PGA**	0.71	0.77
PGV	26.10	40.87	7.55	3.46	8.80	27.95	**PGV**	28.86	34.38
PGD	153.93	27.33	0.82	0.46	2.45	6.80	**PGD**	195.41	16.24
V/A	0.07	0.11	0.05	0.02	0.08	0.09	**V/A**	0.04	0.05
AI	4.81	2.44	0.11	0.07	0.14	0.89	**AI**	22.20	7.75
Ic	0.10	0.07	0.01	0.01	0.01	0.04	**Ic**	0.33	0.17
HI	82.70	127.13	17.68	6.73	23.00	74.23	**HI**	84.30	69.40
Tp	0.50	0.60	0.46	0.08	0.20	0.18	**Tp**	0.12	0.44
Tm	0.38	0.49	0.36	0.14	0.32	0.41	**Tm**	0.21	0.23

Table 2: Significant earthquakes monitored at station CBGS in New Zealand.

Time		Mw
Date	hr:min:sec	
2010-09-03	16:35:41	7.10
2010-09-07	19:49:57	5.13
2010-12-25	21:30:15	4.89
2011-02-21	23:51:42	6.34
2011-02-22	1:50:26	5.91
2011-06-13	1:01:00	5.63
2011-06-13	2:20:49	6.00
2011-12-23	0:58:38	5.80
2011-12-23	2:18:03	6.00

Table 3: Input motion characteristics of Christchurch individual earthquake records measured at station CBGS.

Parameter	1	2	3	4	5	6	7	8	9
PGA	1466.00	1527.69	3453.90	5190.80	4377.70	1936.80	1423.80	1585.90	2294.00
PGV	21.83	8.77	18.14	62.95	33.18	9.40	20.36	16.04	29.53
PGD	10.73	3.58	26.57	23.48	5.52	1.55	5.83	6.38	5.13
V/A	0.15	0.06	0.05	0.12	0.08	0.05	0.14	0.10	0.13
AI	0.55	0.14	0.46	2.63	0.80	0.34	0.43	0.42	0.46
Ic	26927.78	7041.55	17673.59	87090.24	26613.64	13881.63	16748.44	1646.02	17641.47
HI	76.02	20.05	39.32	257.99	116.22	35.59	75.25	61.63	91.28
Tp	0.42	0.30	0.14	0.48	0.20	0.32	0.44	0.38	0.34
Tm	0.81	0.32	0.29	1.05	0.67	0.39	0.79	0.69	0.74

Table 4: First two natural periods of the frame systems.

Frame ID	T1 (sec)	T2 (sec)
Gravity	1.10	0.46
Direct	0.48	0.17
Capacity	0.28	0.09

Table 5: Stiffness, strength and ductility of frame systems.

Frame ID	Stiffness (KN/m)	Strength KN	Ductility m/m
Gravity	93	179	4.80
Direct	670	680	3.93
Capacity	1670	1370	6.90